

Topological invariant in three-dimensional band insulators with disorder

H.-M. Guo

*Department of Physics, Capital Normal University, Beijing 100048, China**and Department of Physics and Astronomy, University of British Columbia, Vancouver, British Columbia, Canada V6T 1Z1*

(Received 30 June 2010; revised manuscript received 30 August 2010; published 27 September 2010)

Topological insulators in three dimensions are characterized by a Z_2 -valued topological invariant, which consists of a strong index and three weak indices. In the presence of disorder, only the strong index survives. This paper studies the topological invariant in disordered three-dimensional system by viewing it as a supercell of an infinite periodic system. As an application of this method we show that the strong index becomes nontrivial when strong enough disorder is introduced into a trivial insulator with spin-orbit coupling, realizing a strong topological Anderson insulator. We also numerically extract the gap range and determine the phase boundaries of this topological phase, which fits well with those obtained from self-consistent Born approximation and the transport calculations.

DOI: [10.1103/PhysRevB.82.115122](https://doi.org/10.1103/PhysRevB.82.115122)

PACS number(s): 73.43.-f, 72.25.Hg, 73.20.-r, 85.75.-d

Time-reversal invariant band insulators of noninteracting electrons are basically divided into two classes: the ordinary insulator and the topological insulator.¹⁻⁴ The latter is a novel phase of quantum matter. It has an insulating bulk gap and gapless edge or surface states. These gapless states are topologically protected and are immune to nonmagnetic disorder. Recently another kind of nontrivial quantum phase termed topological Anderson insulator (TAI) has been predicted to exist in two dimensions (2D) (Refs. 5-7) and three dimensions (3D),⁸ which makes the situation more interesting. In the TAI phase, remarkably, the topologically protected gapless states emerge due to disorder.

For systems without disorder, the topological phases can be characterized by studying the gapless states as obtained, e.g., from diagonalizing the Hamiltonian in a geometry with edges or surfaces. They can also be characterized by the topological invariants calculated from the bulk Hamiltonian, which have been well studied in recent literature.^{9,10} However in the disordered systems, gapless modes alone cannot unambiguously identify the topological phases because they may be localized in space. Instead, the transport properties are usually used to find these extended topologically protected modes. Similarly we may also use the topological invariant to characterize the topological phases induced by disorder. A question naturally arises: how to calculate the topological invariant in the presence of disorder.

At first glance, it is not obvious how to generalize the present methods from translation invariant band insulators to the disordered systems. Let us first recall the integer quantum Hall effect (IQHE) where the generalization to the case with disorder is well understood. The topological quantum number in IQHE, which characterizes the quantized Hall conductivity, is known as the first Chern number [also referred to as the Thouless-Kohmoto-Nightingale-den Nijs (TKNN) integer]¹¹ and is closely related to Berry's phase. In the presence of disorder, the TKNN integers defined for a clean system can be generalized. By introducing generalized periodic boundary conditions and averaging over different boundary condition phase, an invariant expression can be constructed applicable to the situation where many-body interaction and substrate disorder are present.^{12,13} Since the boundary condition phases can be transferred to the Hamil-

tonian by a unitary transformation, such considerations are actually equivalent to thinking of the system as a supercell of an infinite system. Since the infinite system which is periodic in the supercell has translation symmetry, the wave vectors can be well defined, which, in fact, correspond to the boundary condition phases. The advantage of such consideration is that since the band structure is recovered, one can use the known methods to calculate the topological invariant for the infinite system. The finite system under consideration, which is now a supercell of the infinite system, shares the same topological properties as the infinite system. This idea has been used to study the phase transition in the presence of disorder in 2D quantum spin Hall system (QSHE),¹⁴ where the authors found that a metallic region always appears between ordinary and topological insulators in spin-orbit coupled systems with disorder when there is no extra conservation law (recently the same result is also obtained via C^* -Algebras¹⁵).

In this paper, we study the topological invariant of the disordered 3D system by viewing it as a supercell of an infinite system. We start from a trivial insulator with spin-orbit coupling and find that when strong enough disorder is introduced into the system, a gap appears at half filling and the corresponding topological invariant is nontrivial, confirming the existence of the disorder-induced nontrivial topological phase.

To be concrete, we consider a model describing itinerant electrons with spin-orbit coupling on a cubic lattice with the Hamiltonian in the momentum space,^{16,17}

$$H(\mathbf{k}) = d_4(\mathbf{k})I_{4 \times 4} + \begin{pmatrix} d_0(\mathbf{k}) & d_3(\mathbf{k}) & 0 & d_-(\mathbf{k}) \\ d_3(\mathbf{k}) & -d_0(\mathbf{k}) & d_-(\mathbf{k}) & 0 \\ 0 & d_+(\mathbf{k}) & d_0(\mathbf{k}) & -d_3(\mathbf{k}) \\ d_+(\mathbf{k}) & 0 & -d_3(\mathbf{k}) & -d_0(\mathbf{k}) \end{pmatrix}, \quad (1)$$

where $d_{\pm}(\mathbf{k}) = d_1(\mathbf{k}) \pm id_2(\mathbf{k})$, $d_0(\mathbf{k}) = \epsilon - 2t\sum_i \cos k_i$, $d_i(\mathbf{k}) = -2\lambda \sin(k_i)$, and $d_4(\mathbf{k}) = 2\gamma(3 - \sum_i \cos k_i)$ ($i=1,2,3$). This Hamiltonian is a lattice version of the effective low-energy Hamiltonian describing the physics of insulators in Bi_2Se_3

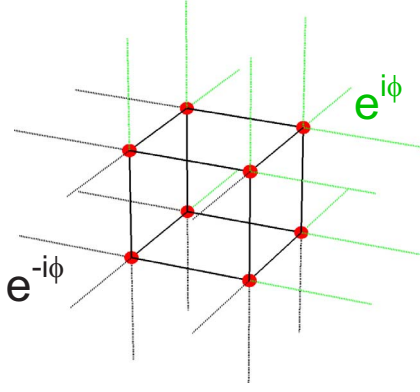


FIG. 1. (Color online) The cubic lattice on which the Hamiltonian is defined. As an example, the supercell has a size 2^3 (red closed circles). The sites which have connections with next (previous) supercell obtain phases $e^{i\phi_i}$ ($e^{-i\phi_i}$), where $\phi_i=0$ or π and $i=x,y,z$ depends on the TRIM and the direction of the bonds.

family.^{18–21} At half filling, depending on the parameters, the system can be a trivial insulator or a topological insulator. To simulate the effects of disorder we consider a random on-site potential $\sum_j U_j \Psi_j^\dagger \Psi_j$ with U_j uniformly distributed in the range $(-U_0/2, U_0/2)$. This kind of disorder respects time-reversal symmetry. The lattice on which the Hamiltonian resides is a cubic lattice with a finite size $L_x \times L_y \times L_z$ (the lattice constant $a=1$). There is no translation symmetry in the system when disorder is present. However taking the system as a supercell of an infinite system, translation symmetry is recovered. The lattice vector becomes $\mathbf{a}'_i = L_i$ (the size of the supercell in $i=x,y,z$ directions) and the corresponding reciprocal lattice vectors are $\mathbf{b}_i = \frac{2\pi}{L_i}$.

In 3D, the topological invariant consists of four Z_2 numbers forming an index $(\nu_0; \nu_1 \nu_2 \nu_3)$, which distinguish 16 topological classes.^{10,22} Usually it is a difficult problem to evaluate them for a given band structure. However in the presence of inversion symmetry, the problem can be greatly simplified. It has been shown that they can be determined from the knowledge of the parity $\xi_{2m}(\Gamma_i)$ of the $2m$ th occupied energy band at the eight time-reversal invariant momenta (TRIM) Γ_i that satisfy $\Gamma_i = \Gamma_i + \mathbf{G}$. The eight TRIM can be expressed in terms of primitive reciprocal lattice vectors as $\Gamma_{i=(n_1 n_2 n_3)} = (n_1 \mathbf{b}_1 + n_2 \mathbf{b}_2 + n_3 \mathbf{b}_3)/2$ with $n_j=0, 1$. Then ν_α is determined by the product $(-1)^{\nu_0} = \prod_{n_j=0,1} \delta_{n_1 n_2 n_3}$ and $(-1)^{\nu_{i=1,2,3}} = \prod_{n_j \neq i=0,1; n_i=1} \delta_{n_1 n_2 n_3}$, where the parity product for the occupied bands $\delta_i = \prod_{m=1}^N \xi_{2m}(\Gamma_i)$. To take advantage of the simplification, we only consider disorder configurations with inversion symmetry. For large enough supercell such consideration will not change the underlying physics. So to calculate the topological invariant, we only need to consider the Hamiltonian at the eight TRIM and they are equivalent to those of a finite system with boundary conditions which are periodic up to phases $\phi_x, \phi_y, \phi_z=0$ or π for boundary sites, as shown in Fig. 1.

To understand what happens when introducing the supercell, we first calculate the Z_2 topological invariant of a clean (1;000) strong topological insulator. The results are shown in Fig. 2(a). At half filling, we find that $\delta = -1$ at the Γ point and $\delta = 1$ at other TRIM. This result is consistent with the ordi-

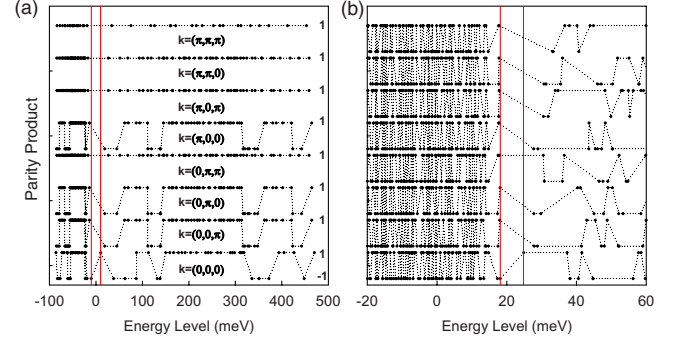


FIG. 2. (Color online) The parity product for the occupied states at the eight TRIM for a 8^3 supercell (a) without disorder and (b) with disorder. The crosses mark the eigenvalue of the system and the corresponding parity product for the filling up to this energy level. Here we use parameters: $t=24$ meV, $\lambda=20$ meV, and $\gamma=16$ meV and (a) $\epsilon=134$ meV, corresponding to $m=-10$ meV, where the system is a (1;000) strong topological insulator; (b) $\epsilon=145$ meV and $U_0=150$ meV, corresponding to $m=1$ meV, where the clean system is a trivial insulator. The red lines in both figures show the gap range which appears at half filling.

nary band-structure calculations and the reason is explained below. Taking a supercell means enlarging the original unit cell in the \mathbf{a}_1 , \mathbf{a}_2 , and \mathbf{a}_3 directions (\mathbf{a}_1 , \mathbf{a}_2 , and \mathbf{a}_3 are the lattice vectors of the original lattice). The resulting new Brillouin zone (BZ) is folded in the corresponding directions and shrunk in size. The occupied states at the eight TRIM for the new BZ contain those at the eight TRIM for the original BZ. Though more states which are at other momenta of the original BZ will reside on the TRIM of the new BZ, they do not change the parity product for the occupied states. Thus the product of all eight δ 's from the supercell calculation still yield the same “strong” index of the Z_2 topological invariant. However the “weak” index cannot be obtained from this method if the supercell contains an even number of unit cell in the corresponding direction. As mentioned above, the weak indices ν_1 , ν_2 , and ν_3 are the product of four δ 's which are in the planes $k_1=\pi$, $k_2=\pi$, and $k_3=\pi$, respectively. Suppose that the supercell contains an even number of unit cell in the \mathbf{a}_1 direction, then the $k_1=0$ and $k_1=\pi$ planes will collapse onto the $k'_1=0$ plane in the new BZ. Thus the weak index determined by the four TRIM on the $k'_1=\pi$ plane in the new BZ must be 0. From another point of view, this is understandable because the weak indices are related to layered 2D quantum spin-Hall states and the 3D supercell naturally fails in calculating the quantities reflecting the 2D physics. When considering systems with disorder, the weak indices are eliminated and only the strong index remains robust. The topological invariant for the system with disorder is the strong index of the Z_2 topological invariant for clean 3D band insulators. In the following, we simply call it the topological invariant for the 3D systems with disorder.

Now we take into account disorder as described above and start from a trivial insulator. Figure 2(b) shows the result of such a calculation on a 8^3 lattice with $U_0=150$ meV. Generally the disorder will eliminate all degeneracies except those protected by time-reversal symmetry. So at the TRIM, each eigenvalue of the Hamiltonian is doubly degenerate.

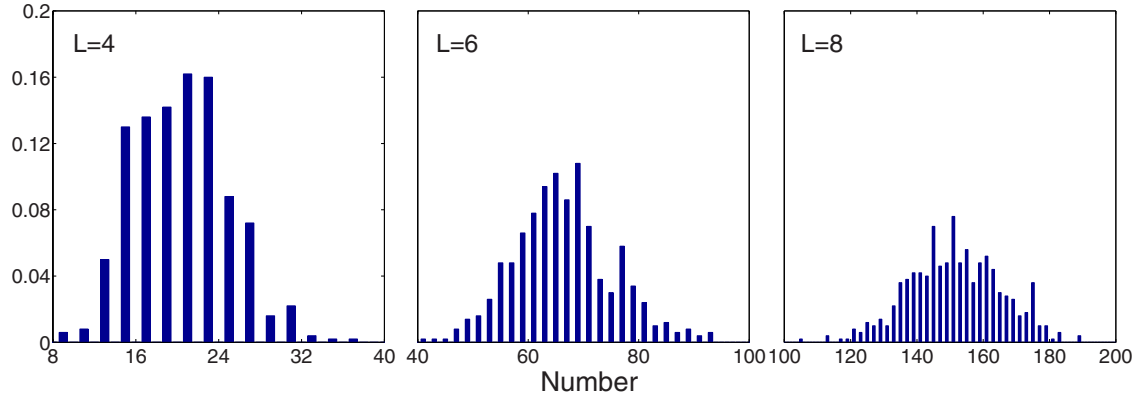


FIG. 3. (Color online) Distributions of the number of Z_2 -odd band pairs from 500 disorder realizations. The bar heights is the fraction of disorder realizations that have a given number of band pairs with $Z_2=1$ (the numbers are all odd here). The parameters are the same as those in Fig. 2(b).

Though the disorder makes the energy spectrum more continuous, a small gap remains clear at half filling. Here the gap location is shifted to the high energy, which is different from the case in the clean system where the gap appears symmetrically at $E=0$. The parity eigenvalue products $\delta=-1$ at the Γ point and $\delta=1$ at other TRIM for half filling show that the topological invariant of the system is 1 so the system will exhibit nontrivial topological properties. We have extended the above calculation to 500 different disorder realizations. In all 500 disorder realizations, the topological invariant is 1 for half filling, which further confirms the topological phase in the system. Thus through calculating the topological invariant of the system, we obtain further confirmation of the topological phase induced by disorder. This new phase has been termed as “strong TAI” (STAI).⁸ Due to the nontrivial topological properties in STAI, topologically protected surface states will appear at the surfaces as the case in the “strong topological insulator” phase of the clean system, which has already been verified by transport calculations.

It is also interesting to look at the number of Z_2 -odd band pairs. In 2D QSHE, the number of Z_2 -odd Kramers pairs increases linearly with the system size in the metallic region and grows slowly for the topological insulator.¹⁴ Here in 3D, we find a similar result. In Fig. 3, we show the distribution of the number of Z_2 -odd band pairs at three lattice sizes 4^3 , 6^3 , and 8^3 . We find that the location of the mean roughly scales with L^3 (L is the lattice size). A detailed analysis on the limited data also shows that the number growth is somewhat slower than linear. With enough data and larger sizes, finite-size scaling could be carried out. However this is not accessible at present due to the limited computer resources.

For different disorder realizations, though there still exists a gap at half filling, its position on the energy axis changes randomly. We extract the energy levels for the most energetic electron at half filling and the one just above it and show their distributions in Fig. 4. The curves in Fig. 4 show Gaussian-type distributions. The distributions for half filling and half plus one at some TRIM have no overlaps while on the other TRIM have overlaps. This means there is no “true” gap range even for the eight TRIM. However the overlaps are already very small for the lattice size of 8^3 . We also

performed the same calculations on lattice sizes of 4^3 and 6^3 . With the increasing lattice size the widths of the distributions decrease. We therefore attribute the overlaps for the present lattice size to finite-size effect and expect them to diminish for larger lattice sizes.

For the parameters used the physical gap size is determined by gap at $\mathbf{k}=(0,0,0)$ TRIM. We can obtain the gap value from the peaks of the distributions and this value will approximate the one for the larger lattice size. We have determined the phase diagram in the U_0-E_F plane from calculations on a 6^3 system and the result is shown in Fig. 5. The range of STAI in the U_0-E_F plane has also been obtained from conductivity calculations and the self-consistent Born approximation (SCBA), where the weak-disorder boundary fits well with each other while the strong-disorder boundary does not.⁸ It was found that the weak-disorder boundary marks the crossing of a band edge and the strong-disorder boundary marks the crossing of a mobility edge, and the SCBA does not work for the strong-disorder boundary.⁷

The result in Fig. 5 shows that the phase boundaries ob-

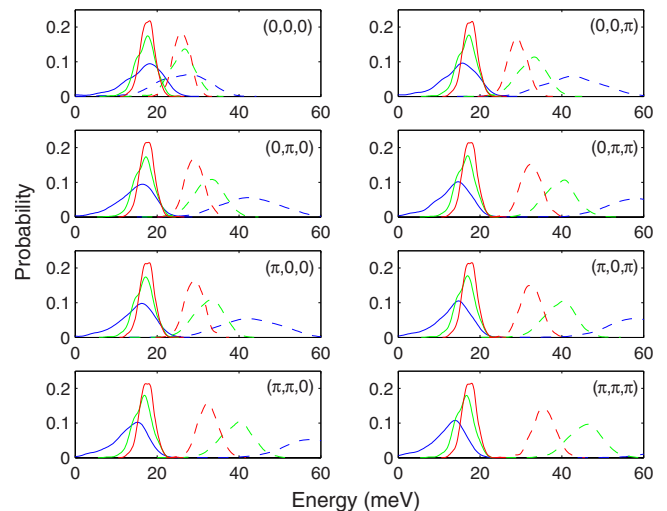


FIG. 4. (Color online) Distributions of energy levels at half filling and half plus one filling from 500 disorder realizations. The system sizes are 4^3 (blue), 6^3 (green), and 8^3 (red). The parameters are the same as those in Fig. 2(b).

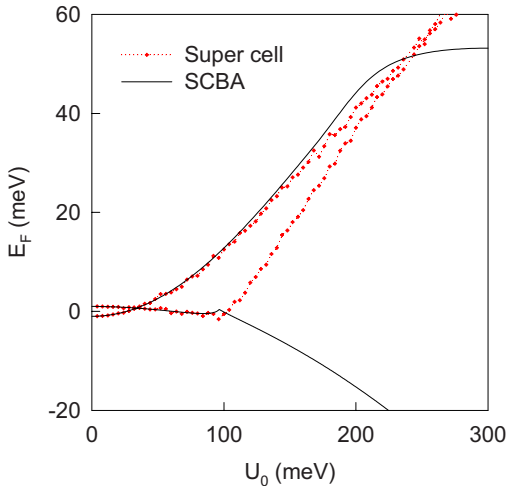


FIG. 5. (Color online) Phase boundaries for the STAI phase in the U_0-E_F plane obtained from the supercell calculations. The red crosses represent the peaks in energy-level distributions for half and half plus one fillings and are obtained from calculations of 500 disorder realizations on 6^3 system. The phase boundaries from the SCBA are also shown for comparison.

tained from the present calculation fits well for both the weak-disorder and strong-disorder phase boundaries determined from the conductivity calculation.⁸ The range of STAI phase should be determined by the gap between the two edges containing extended states. We believe that we have extracted such a gap. The reason is that the localized states are closely related to the disorder realizations and can be removed by an average over disorder realizations. In the phase diagram, increasing the strength of disorder, the system first undergoes a sharp phase transition, which happens at a critical disorder strength where the gap closes. Then the system enters a stable topological phase for a wide range of disorder strength. Finally the system experiences another phase transition to a diffusive metal. Close to the latter transition, the finite system under consideration is in a mixed

phase, where some fraction of disorder realizations yields a nontrivial topological invariant.

In conclusion, we have generalized the method of calculating the topological invariant in disordered 2D QSHE to 3D disordered systems. In this method, the finite 3D system is viewed as a supercell of a large lattice with well-defined wave vector, which allows us to directly use the definition of topological invariants for clean band insulators. The obtained topological invariant can be thought of as describing the finite system with disorder. Using the inversion symmetry preserving disorder configurations, we carried out explicit calculations on a model Hamiltonian (describing the physics of insulators in Bi_2Se_3 family) with on-site disorder. We found that the topological invariant for a system that is a trivial insulator in the absence of disorder can become nontrivial when strong enough disorder is introduced. This result confirms the existence of the strong topological Anderson insulator, a topological phase in three space dimensions whose existence is fundamentally dependent on disorder.⁸

As additional application of this method we counted the number of Z_2 -odd band pairs. Though this number varies with the disorder realization, the total number is always odd when the system is in the STAI phase and it scales roughly linearly with the number of the lattice sites. Finally, we obtained the phase boundaries for the STAI phase by extracting the gap range, which fits well with the known results.

In the presence of on-site disorder, the diagonal elements of the Hamiltonian matrix are random, drawn from a statistical distribution. The Hamiltonian can be regarded as a random matrix which can be studied in the framework of the random matrix theory (RMT). The RMT has already been applied to IQHE and disordered superconductors.²³⁻²⁵ We expect some insights into the present problem from RMT, which we leave to future work.

The authors are indebted to I. Garate, M. Franz, G. Refael, G. Rosenberg, C. Weeks, and M. Vazifeh for stimulating discussions. Support for this work came from NSERC, CIFAR, and the China Scholarship Council.

¹B. A. Bernevig, T. L. Hughes, and S.-C. Zhang, *Science* **314**, 1757 (2006).

²J. E. Moore, *Nature (London)* **464**, 194 (2010).

³M. Z. Hasan and C. L. Kane, [arXiv:1002.3895](https://arxiv.org/abs/1002.3895) (unpublished).

⁴X.-L. Qi, T. L. Hughes, and S.-C. Zhang, *Phys. Rev. B* **78**, 195424 (2008).

⁵J. Li, R.-L. Chu, J. K. Jain, and S.-Q. Shen, *Phys. Rev. Lett.* **102**, 136806 (2009).

⁶H. Jiang, L. Wang, Q.-F. Sun, and X.-C. Xie, *Phys. Rev. B* **80**, 165316 (2009).

⁷C. W. Groth, M. Wimmer, A. R. Akhmerov, J. Tworzydło, and C. W. J. Beenakker, *Phys. Rev. Lett.* **103**, 196805 (2009).

⁸H.-M. Guo, G. Rosenberg, G. Refael, and M. Franz, [arXiv:1006.2777](https://arxiv.org/abs/1006.2777) (unpublished).

⁹J. E. Moore and L. Balents, *Phys. Rev. B* **75**, 121306(R) (2007).

¹⁰L. Fu and C. L. Kane, *Phys. Rev. B* **76**, 045302 (2007).

¹¹D. J. Thouless, M. Kohmoto, M. P. Nightingale, and M. den Nijs, *Phys. Rev. Lett.* **49**, 405 (1982).

¹²Q. Niu, D. J. Thouless, and Y.-S. Wu, *Phys. Rev. B* **31**, 3372 (1985).

¹³J. E. Avron and R. Seiler, *Phys. Rev. Lett.* **54**, 259 (1985).

¹⁴A. M. Essin and J. E. Moore, *Phys. Rev. B* **76**, 165307 (2007).

¹⁵T. A. Loring and M. B. Hastings, [arXiv:1005.4883](https://arxiv.org/abs/1005.4883) (unpublished).

¹⁶P. Hosur, S. Ryu, and A. Vishwanath, *Phys. Rev. B* **81**, 045120 (2010).

¹⁷G. Rosenberg and M. Franz, *Phys. Rev. B* **82**, 035105 (2010).

¹⁸H. Zhang, C.-X. Liu, X.-L. Qi, X. Dai, Z. Fang, and S.-C. Zhang, *Nat. Phys.* **5**, 438 (2009).

¹⁹Y. Xia, D. Qian, D. Hsieh, L. Wray, A. Pal, H. Lin, A. Bansil, D. Grauer, Y. S. Hor, R. J. Cava, and M. Z. Hasan, *Nat. Phys.* **5**, 398 (2009).

- ²⁰Y. L. Chen, J. G. Analytis, J.-H. Chu, Z. K. Liu, S.-K. Mo, X. L. Qi, H. J. Zhang, D. H. Lu, X. Dai, Z. Fang, S. C. Zhang, I. R. Fisher, Z. Hussain, and Z.-X. Shen, *Science* **325**, 178 (2009).
- ²¹D. Hsieh, Y. Xia, D. Qian, L. Wray, F. Meier, J. H. Dil, J. Osterwalder, L. Patthey, A. V. Fedorov, H. Lin, A. Bansil, D. Grauer, Y. S. Hor, R. J. Cava, and M. Z. Hasan, *Phys. Rev. Lett.* **103**, 146401 (2009).
- ²²H.-M. Guo and M. Franz, *Phys. Rev. Lett.* **103**, 206805 (2009).
- ²³D. J. E. Callaway, *Phys. Rev. B* **43**, 8641 (1991).
- ²⁴M. Janssen and K. Pracz, *Phys. Rev. E* **61**, 6278 (2000).
- ²⁵S. R. Bahcall, *Phys. Rev. Lett.* **77**, 5276 (1996).